ISSN 1027-4510, Journal of Surface Investigation: X-ray, Synchrotron and Neutron Techniques, 2022, Vol. 16, No. 6, pp. 1081–1088. © Pleiades Publishing, Ltd., 2022.

Dynamics of Elemental and Phase Composition of the Surface of AK5M2 Alloy Modified with Ti and Irradiated by an Electron Beam

A. A. Serebryakova[a], *, D. V. Zaguliaev[a], Yu. A. Shliarova[a], Yu. F. Ivanov[b], and A. M. Ustinov[c]

[a] *Siberian State Industrial University, Novokuznetsk, 654007 Russia*

[b] *Institute of High Current Electronics, Siberian Branch, Russian Academy of Sciences, Tomsk, 634055 Russia*

[c] *Tomsk State University of Architecture and Building, Tomsk, 634003 Russia*

**e-mail: aserebrakova87@gmail.com*

Received March 15, 2022; revised May 25, 2022; accepted May 25, 2022

Abstract—The surface layer of AK5M2 alloy is modified with a Ti film by the vacuum-arc method. The modified samples are irradiated by the method of electron-beam processing using five modes. The dependences of the crystal-lattice parameter and the phase composition of samples of the AK5M2 alloy with surface-modified Ti alloy on the beam energy density during electron-beam processing are determined. The defect substructure of the samples is studied by scanning electron microscopy. The dependence of the coating thickness on the energy density of the electron beam is revealed. The modes are determined, in which the electron-beam energy density is insufficient for the formation of a homogeneous coating. The most rational mode of electron-beam processing is established, in which a homogeneous layer with the least number of surface defects is formed.

Keywords: composite material, electron-beam processing, X-ray phase analysis, AK5M2 alloy

DOI: 10.1134/S1027451022060222

INTRODUCTION

Increasing the strength properties of the surface layers of light metals and alloys, such as silumin [1, 2], is quite topical at present [3]. This is due to the wide use of these alloys in the automotive [4–6] and aerospace industries [7]. The operation of parts made of metals and alloys implies a constant load on their surface. It is known that the destruction of parts begins with the formation of surface-layer defects (cracks, microdepressions and other defects), which is the reason for an increase in requirements for the properties and characteristics of the surface layer. The characteristics that determine the efficiency of the surface layer of products are strength and hardness of the processing surface, uniformity of the structure and properties, high fracture resistance, and resistance to cracking [8]. Currently, in the field of condensed matter physics, much attention is paid to improving the properties of metals and alloys by the use of external energy effects [9, 10]. Surface-modification methods are classified according to the type of external impact: ion beams, plasma, ultrasound etc. One of the most efficient and environmentally friendly methods is electron-beam processing [11–13]. The advantages of such processing compared to other modification methods are a high energy efficiency, higher energy-density uniformity over the flow cross section, good pulse reproducibility and high pulse-repetition rate.

The method of doping the surface layer by the deposition of a thin film on the surface of the material and subsequent remelting of the film with the surface layer (substrate) as a result of electron-beam irradiation is also applied [14]. On the basis of current research, it was established [15–19] that the greatest effect in modifying the surface layers of metals and alloys can be achieved due to complex processing and a combination of energy-impact methods. A variant of complex processing is the combination of doping by the deposition of a film on the surface of the material under study by ion-plasma sputtering followed by remelting of the modified layer by an electron beam. The use of these innovative processing methods makes it possible to increase the strength properties of the surface of materials and alloys.

This work is topical, since its purpose is to study the effect of the electron-beam irradiation of an AK5M2 alloy with a surface-modified Ti layer, namely, a change in the elemental and phase composition, crystal-lattice parameters and surface structure.

EXPERIMENTAL

AK5M2 Alloy was chosen as the material for study. Samples with a size of 10 × 20 × 20 mm (Fig. 1) for electron-beam processing, X-ray phase analysis and

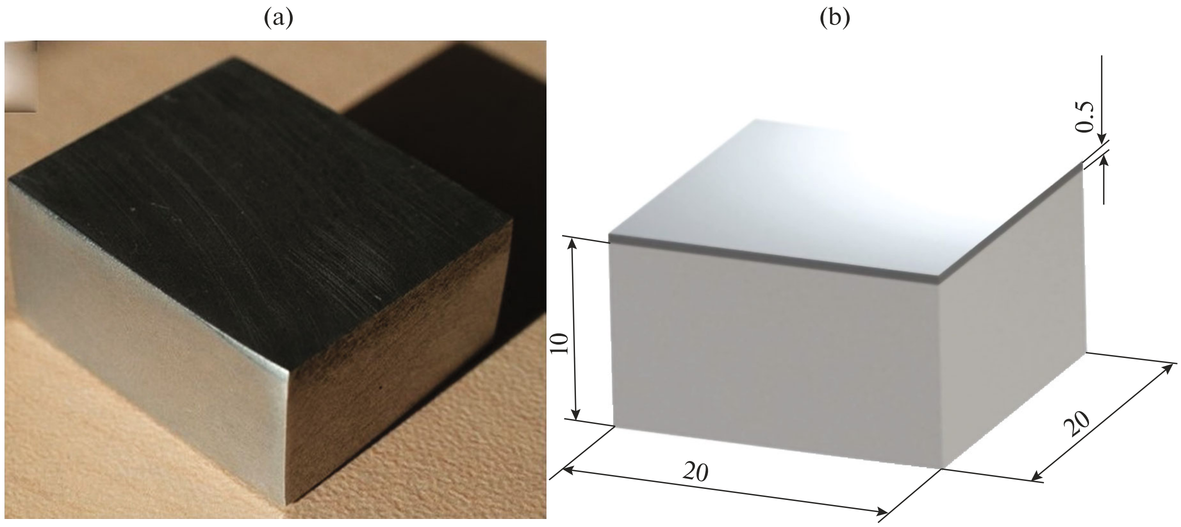

Fig. 1. Sample AK5M2 in the cast state (a) and surface-modified with Ti (b). All dimensions are in mm.

scanning electron microscopy (SEM) were a system of a substrate made of AK5M2 alloy and a Ti film.

The composite material was formed by the vacuum-arc method on a KVINTA automated vacuum ion-plasma setup [20]. A titanium film 0.5 μm thick (Fig. 1b) was deposited onto the samples of the AK5M2 alloy using an arc evaporator with the following process parameters: the samples were located opposite the arc evaporator, deposition was carried out without sample rotation, the current of the arc evaporator was I_A = 80 A (electrodynamic resistance current), startup current was I_S = 20 A, nominal current was I_N = 135 A, γ = 75%, bias voltage was U_{bias} = 35 V, p = 0.3 Pa, and t = 10 min.

Irradiation with a pulsed electron beam was carried out on a Solo setup [21]. During the experiment, the parameters of the setup during irradiation were as follows: the energy of accelerated electrons was U = 17 keV, the energy density of the electron beam E_S was controlled in five modes: no. 1, 10; no. 2, 20; no. 3, 30; no. 4, 40; no. 5, 50 J/cm^2. The pulse duration was τ = 200 μs, number of pulses was n = 3, pulse-repetition rate was f = 0.3 s^{-1}, and the residual gas pressure (argon) in the working chamber of the setup was p = 2 × 10^{-2} Pa. The choice of modes of electron-beam processing presented in the work is due to a wide range of studies that have confirmed in practice the effectiveness of these parameters in comparison with others. The results of studies carried out on silumin modified with the Al–Y_2O_3 system indicate the high efficiency of these parameters due to an increase in microhardness and wear resistance [22].

The surface was studied by SEM methods [23–25] using a Philips SEM-515 device with an EDAX ECON IV microanalyzer. X-ray phase analysis [26] was performed using a Shimadzu XRD 6000 diffractometer.

MAIN RESULTS

Results of X-ray Phase Analysis

The qualitative and quantitative phase composition shows a diverse distribution of elements on the surface of the material, depending on the processing mode. The main phases in the initial state of the AK5M2 alloy are a solid solution based on Al and Si, one of which is a phase of the composition Si_3N_4.

The composition presented by Al, Si and Ti phases is found in the X-ray phase analysis of the AK5M2 alloy with surface-modified Ti followed by electron-beam irradiation in mode no. 1. In mode no. 2, the phase composition is presented by Al and Ti; the Al_3Ti phase is additionally revealed. The Al and Al_3Ti phases are found when the energy density of the electron beam increases in mode no. 3. With a further increase in the energy density of the electron beam in mode no. 4, the phase composition is represented exclusively by the Al phase. When examining a sample after processing in mode no. 5, the Al and Al_3Ti phases are found as well as the CuO phase. Thus, with an increase in the energy of the electron beam due to high-speed, high-temperature melting, the materials of the film and substrate are mixed. As a result, the Si phase dissolves in the aluminum solid solution and is not detected in the X-ray phase analysis of the samples processed in modes nos. 2–5. Mixing of the film and substrate material also affects the detection of the CuO phase in mode no. 5. Being initially in the composition of the AK5M2 alloy, the CuO phase comes to the surface of the formed system during high-temperature electron-beam processing.

For the Al and Al_3Ti phases, the crystal-lattice parameters of the AK5M2 alloy with surface-modified Ti followed by electron-beam irradiation are determined by X-ray phase analysis methods. The changes

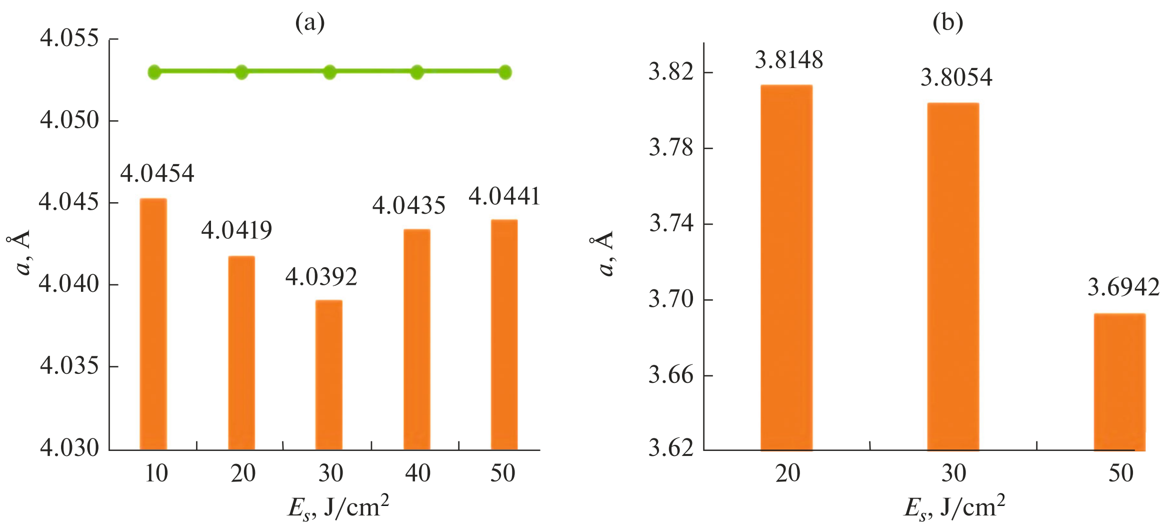

Fig. 2. Crystal-lattice parameters of Al (a) and Al_3Ti (b) phases.

were revealed in comparison with the initial cast state of the AK5M2 alloy (Fig. 2). Figure 2a shows the change in the crystal-lattice parameter of the aluminum phase depending on the processing mode. It can be seen from the obtained data that, in the cast state, the lattice parameter of the AK5M2 alloy is $a = 4.0531$ Å. When processing is applied, the lattice constant decreases in comparison with that of the initial state in all modes. The smallest lattice constant is found in mode no. 3 and it is $a = 4.0392$ Å. As a rule, with a decrease in the crystal-lattice parameter, its compaction occurs, which, in turn, can lead to changes in the properties of the material under study.

Figure 2b shows the dynamics of the crystal-lattice parameter of the Al_3Ti phase, which is revealed only in three of the five processing modes. As shown in the diagram, the formation of the Al_3Ti phase is facilitated by processing modes with an electron-beam energy density of $E_S = 20$ ($a = 3.8148$ Å), 30 ($a = 3.8054$ Å) and 50 J/cm^2 ($a = 3.6942$ Å). As the E_S value increases, the lattice parameter of the Al_3Ti phase decreases. Presumably, the decrease in the crystal-lattice parameters of the detected Al3Ti phase is associated with an increase in the interatomic binding energy during an increase in the melting temperature with an increase in the energy density of the electron beam (Fig. 2b). Melting of the material at higher temperatures leads to aging of the metal due to the release of secondary phases. As a result, the crystal-lattice parameter decreases, and dispersion strengthening of the material occurs.

SEM Results

The SEM results made it possible to analyze the surface structure of samples of the AK5M2 alloy surface-modified with Ti. Characteristic images of the structure of transverse sections and the surface of the alloy sample under study, which demonstrate the morphologically diverse nature of the material, are shown in Figs. 3–7. We take a closer look at the images for each processing mode.

Figure 3 shows a SEM image of a transverse section of an AK5M2 alloy sample surface-modified with Ti. The samples were processed with an electron beam in five modes with increasing electron-beam density: 10 (Fig. 3a), 20 (Fig. 3b), 30 (Fig. 3c), 40 (Fig. 3d), and 50 J/cm^2 (Fig. 3e). When analyzing the image data, it can be noted that with an increase in the density of the electron energy beam, the structure of the sample becomes more uniform (Figs. 3c, 3d). At lower electron-beam densities, a larger amount of intermetallic compounds (Fig. 3b) and micropores (Fig. 3a) is observed in the structure of the surface layer. The coating thickness changes in various processing modes. During electron-beam processing in mode no. 1 (Fig. 3a) the layer thickness is about 30 μm; in mode no. 2, 30–40 μm (Fig. 3b); no. 3, 40–50 μm (Fig. 3c); mode no. 4, 55–75 μm (Fig. 3d); and no. 5, 80–100 μm (Fig. 3e). After analysis of the thickness of the modified layer, one can note that the thickness increases with increasing energy density of the electron beam.

Figure 4 shows SEM images of the surface of the Ti-modified AK5M2 alloy followed by electron-beam irradiation with different densities in five established modes. Figures 4a and 4b show the surface of a composite material with light gray and white droplets as well as microcraters. Energy dispersive analysis shows that this is a film layer consisting of Ti atoms, which, under the impact of electron-beam processing at 10 and 20 J/cm^2, begins to dissolve gradually in the substrate layer. Incomplete dissolution of the titanium film on the substrate surface is due to the energy of the electron beam, which is insufficient for high-tempera-

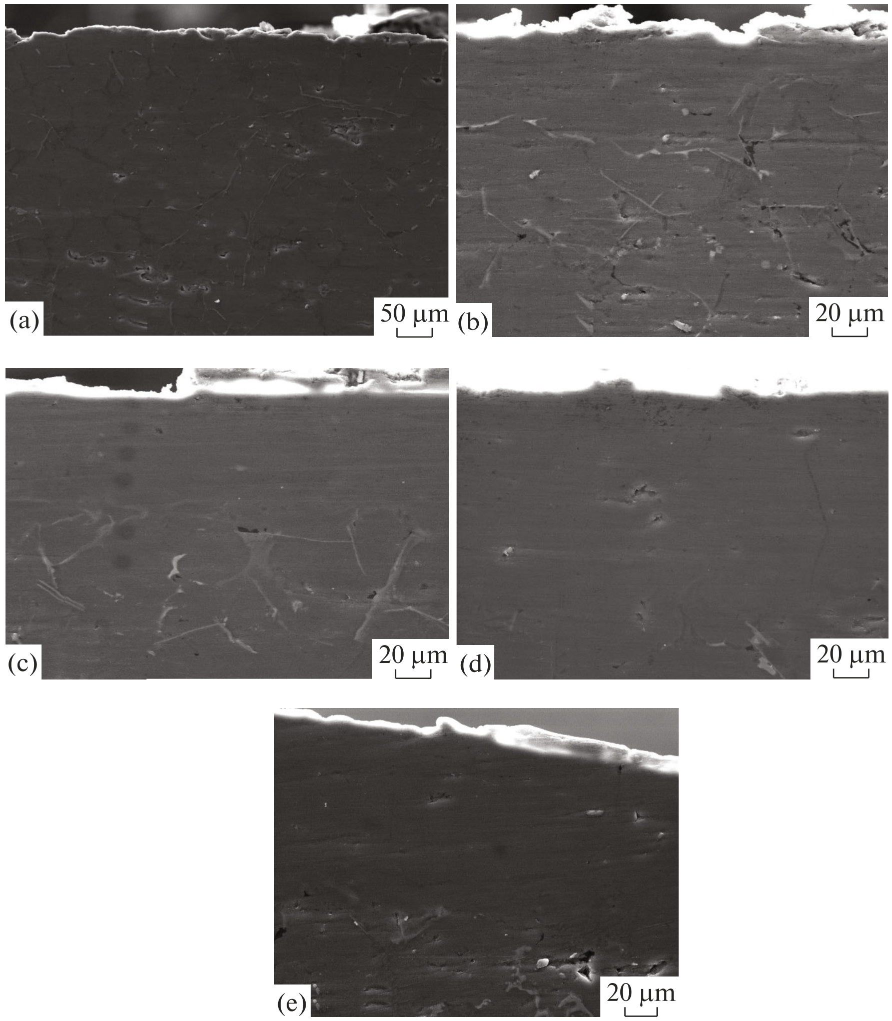

Fig. 3. Changes in the structure of transverse sections of samples of the AK5M2 alloy surface-modified with Ti after electron-beam processing with the electron-beam energy density: (a) 10; (b) 20; (c) 30; (d) 40; (e) 50 J/cm^2.

ture remelting of the entire volume of the deposited titanium film. Figure 4c shows the surface after irradiation with an electron beam with an energy density of 30 J/cm^2; one can note the absence of a Ti droplet fraction on the surface and the fact that the structure became uniform. Figure 4d and 4e shows the state of the surface of the composite material after electron-beam processing with a beam density of 40 and 50 J/cm^2. It is possible to detect large cracks, the origin of which can be strong remelting of the material due to heating to a high temperature during processing, as well as drastic cooling of the material after it.

Table 1. Microanalysis of a titanium droplet

Element	wt %	at %
AlK	14.26	22.68
SiK	01.38	02.10
TiK	82.25	73.70
FeK	00.98	00.75
CuK	01.13	00.76
Matrix	Correction	ZAF

Figure 5 shows the Ti-modified surface of AK5M2 silumin irradiated by an electron beam with an energy density of $E_S = 10$ J/cm^2 (Figs. 5a, 5b). There is a slight fragmentation of the surface by grain boundaries; the grain size is from 80 to 200 μm (indicated by arrows in Fig. 5a). Particles of a droplet fraction of light gray color (titanium) with sizes from 1 to 20 μm are visible (Fig. 5b). In Fig. 5b, a titanium droplet is marked with a cross; according to the microanalysis of its composition, the Ti content is 82.25% (Table 1). According to the results of the X-ray phase analysis of the surface, the content of Al is 84.14%, that of Si is 3.51%, and that of Ti is 12.35%.

In the case of electron-beam processing with increasing energy of the electron beam to E_S = 20 J/cm^2, a

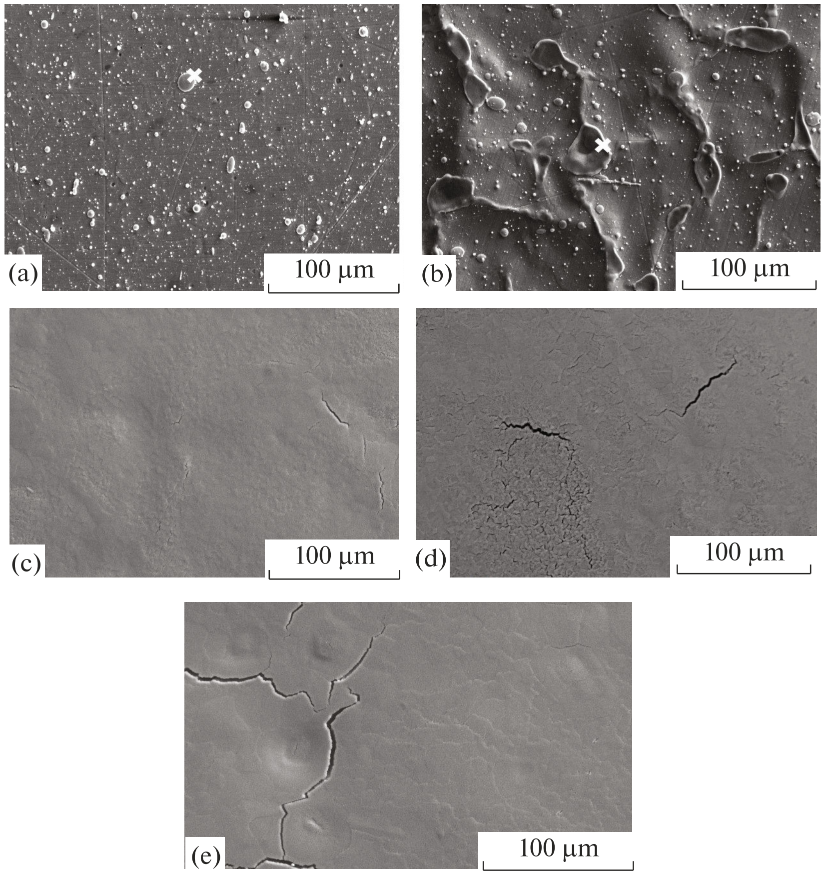

Fig. 4. Surface structure of samples of AK5M2 alloy surface-modified with Ti followed by electron-beam irradiation in five modes of electron-beam processing with the energy density: (a) 10; (b) 20; (c) 30; (d) 40; (e) 50 J/cm^2.

finely fragmented surface structure can be observed. The surface composition includes droplets (Fig. 5d) and microcraters (Fig. 5c). The droplet fractions are smaller than in the previous processing mode, which indicates the gradual formation of a uniform film and substrate structure as the electron-beam density increases. According to the results of X-ray phase analysis, the content of Al is 85.80%, Ti is 12.88%, and Al_3Ti is 1.33%.

Figure 6 shows the alloy AK5M2 surface-modified with Ti and irradiated with an electron-beam energy density of E_S = 30 J/cm^2. A more uniform surface structure is observed compared to the previous results of electron-beam processing. There are no droplet fractions and pronounced cracks; the titanium film is uniformly dissolved on the surface of the AK5M2 silumin substrate (Fig. 6a). A cellular structure is formed (Fig. 6b) with a cell size of about 1 μm. According to the results of the X-ray phase analysis, the content of Al is 99.31%, and that of Al_3Ti is 0.69%.

Figure 7 demonstrates the features of the surface structure of the AK5M2 alloy surface-modified with Ti after irradiation in modes 4 and 5 with an increase in the electron-beam energy density to E_S = 40 J/cm^2 (Figs. 7a, 7b) and then to the maximum value E_S = 50 J/cm^2 (Fig. 7c). Cracks (Fig. 7a), craters and droplets (Fig. 7b) are observed on the surface. A crack about 40 μm in length is clearly visible (Fig. 7c). An increase in the number and size of cracks in the material with an increase in the energy of the electron beam is presumably associated with the processes occurring during high-temperature impact on the surface of the material. As a result of electron-beam processing with energy densities over 30 J/cm^2 melting of the surface layer and its subsequent high-speed crystallization occurs. Due to this, microcracks of various lengths and sizes are formed [26]. X-ray phase analysis made it possible to establish that there is only a solid solution of Al (content of 100%) in this mode of electron-beam processing.

Under the conditions of processing with the maximum energy of the electron beam, the largest number of cracks was found compared to the previous processing modes, e.g., as in Fig. 7c. Cracks divide the structure into fragments of various sizes; intense remelting of the material occurs under the influence of electron beam processing. The structure becomes cellular with a cell size of about 0.5 μm (Fig. 7c). The cracks indi-

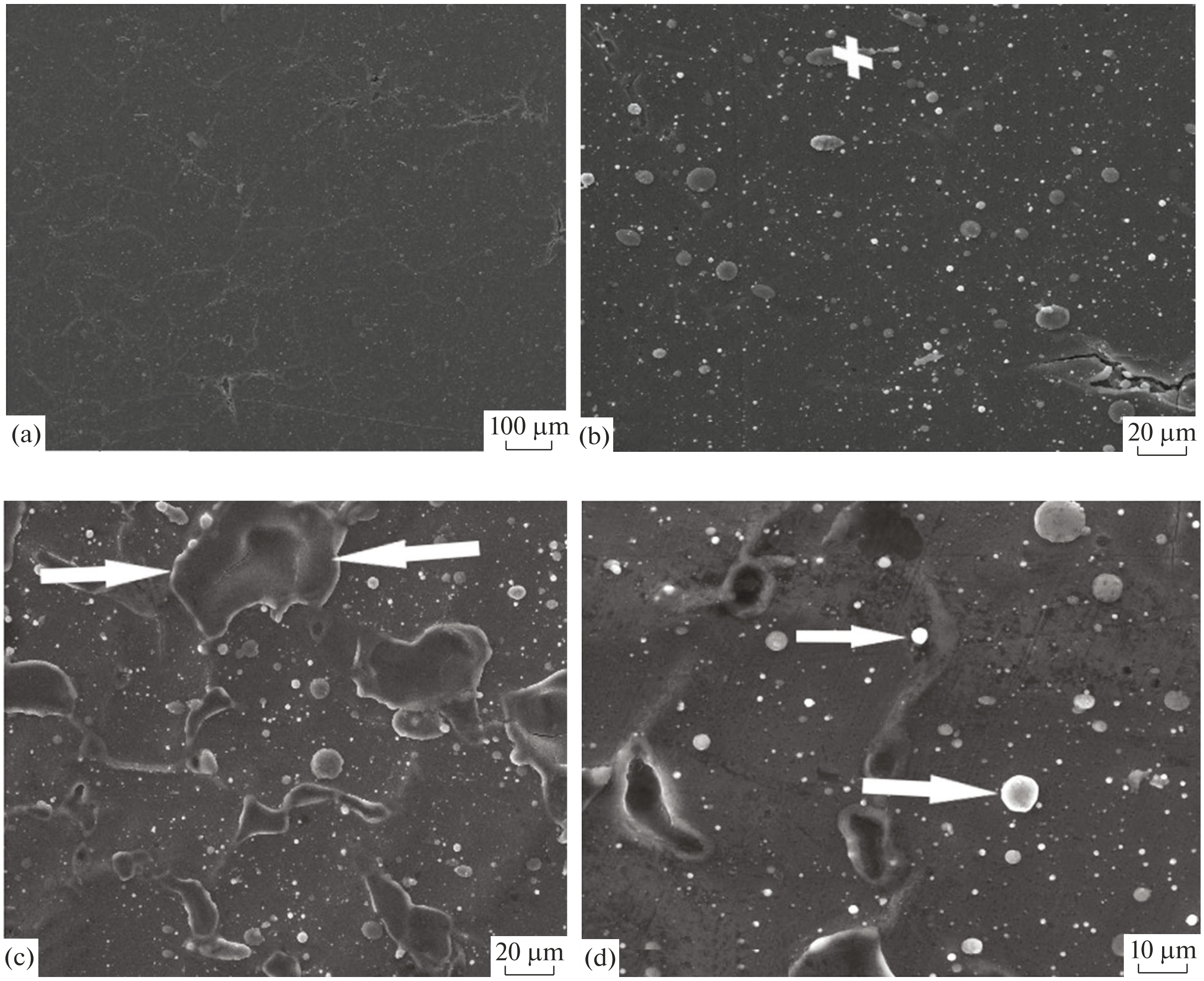

Fig. 5. Structural features of the AK5M2 alloy with a surface-modified Ti layer subjected to electron-beam processing: (a) is surface fragmentation by grain boundaries, $E_S = 10$ J/cm^2; (b) is particles of a droplet fraction of light gray color (titanium), $E_S = 10$ J/cm^2; (c) is microcraters on the surface, $E_S = 20$ J/cm^2; and (d) is finely fragmented surface structure, $E_S = 20$ J/cm^2.

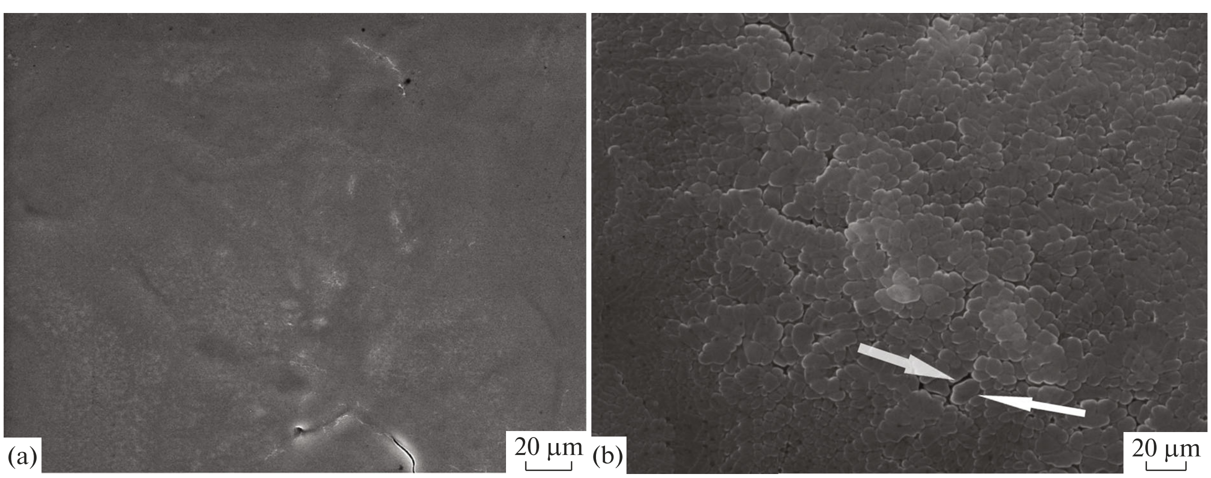

Fig. 6. Structure of the AK5M2 alloy with a surface-modified Ti layer subjected to electron-beam processing ($E_S = 30$ J/cm^2): (a) is uniform dissolution of the titanium film on the substrate surface; (b) is the cellular structure.

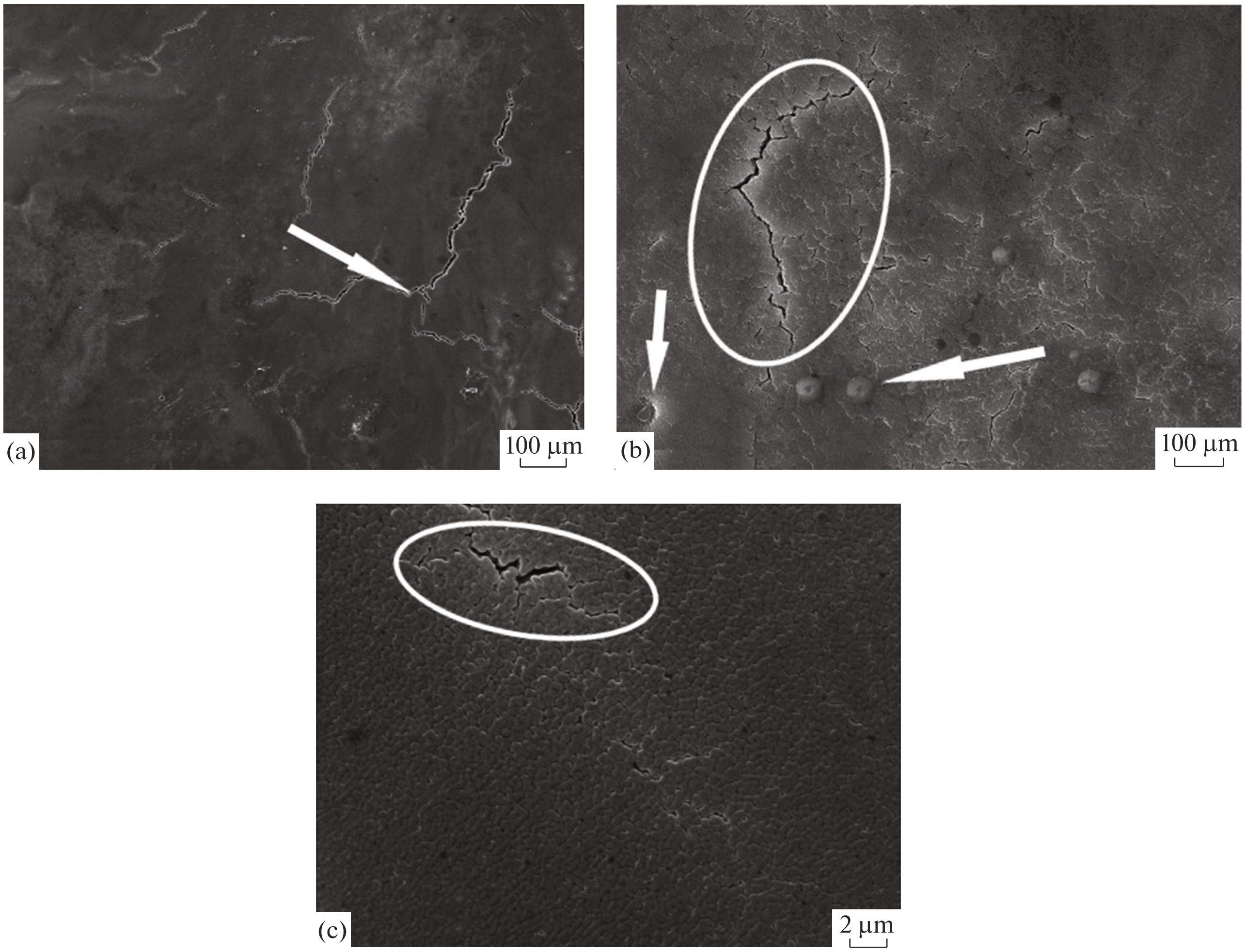

Fig. 7. Structural features of the AK5M2 alloy with a surface-modified Ti layer subjected to electron-beam processing: (a) is cracks on the surface, $E_S = 40$ J/cm^2; (b) is craters and droplets on the surface, $E_S = 50$ J/cm^2; (c) is a crack on the surface with a length of about 40 μm, $E_S = 50$ J/cm^2.

cate that this mode is unsuitable for improving the surface morphology of the AK5M2 alloy, since the surface is fragmented by a large number of microcracks, which, in the case of product operation, are centers of fracture development.

CONCLUSIONS

As a result of X-ray phase analysis of the alloy with a deposited titanium film and subsequent electron-beam processing in five modes, the Al, CuO, and Al_3Ti phases were revealed. The Al_3Ti phase was revealed only during processing in three modes: 2, 3 and 5.

It has been established that irradiation with an electron beam leads to a decrease in the lattice period of the Al phase. However, the dependence of the crystal-lattice period of the Al phase on the energy density of the electron beam E_s is nonlinear, namely, as E_s increases to 30 J/cm^2 it monotonically to the minimum: $a = 4.0392$ Å. A further increase in E_s to 50 J/cm^2 leads to an increase in the lattice period up to $a = 4.0441$ Å. The dependence of the crystal-lattice period of the Al_3Ti phase on the electron-beam density is inversely proportional: with increasing E_s, the period decreases. The supposed reason for the decrease in the lattice parameter is an increase in the temperature of the melting process during electron-beam processing.

Based on SEM analysis of a transverse section of the AK5M2 alloy with surface-modified Ti, a direct dependence of the thickness of the modified layer on the energy density of the electron beam was established. The greater the density, the greater the thickness of the layer.

The dynamics of the surface morphology after electron-beam processing was analyzed. In modes 1 and 2, on the surface of the Ti-modified AK5M2 alloy, SEM analysis revealed incompletely dissolved titanium droplets, which indicates an insufficient energy density of the electron beam to form a uniform coating. Modes 4 and 5, characterized by high electron-beam energy densities, on the contrary, lead to excessive high-temperature remelting of the material. This process contributes to the formation of craters, cracks, micropits on the surface and in the material layer and can lead to destruction of the material during operation.

Thus, based on the results of X-ray phase analysis and SEM of the AK5M2 alloy after the deposition of a titanium film on its surface with various subsequent processing by an electron beam, a mode was established in which a homogeneous fine-grained structure without cracks, micropits and other defects is formed. Obviously, this exposure mode (mode 3) leads to significant transformation of the material properties in the direction of their improvement.

FUNDING

The work was supported by the Russian Science Foundation (project no. 19-79-10059).

CONFLICT OF INTEREST

We declare that we have no conflicts of interest.

REFERENCES

1. B. Otani, J. Inst. Met. **36**, 1926 (2022).
2. *GOST* (State Standard) *R 55375-2012: Primary Aluminum and Alloys Based on It. Grades* (Standartinform, Moscow, 2013).
3. Stetsenko, Lit'e Metall. **1**, 12 (2020). https://doi.org/10.21122/1683-6065-2020-1-18-20
4. Adv. Kurien, Mater. Processes **170**, 28 (2012).
5. Ch. Goenka, R. Nihal, P. Ramanathan, and A. Gupta, Parashar, and J. Joel, Mater. Today: Proc. **22**, 2525 (2020). https://doi.org/10.1016/j.matpr.2020.03.381
6. M. Javidani and D. Larouche, Int. Mater. Rev. **59**, 3 (2014). https://doi.org/10.1179/1743280413Y.0000000027
7. F. Robles Hernández, J. Herrera Ramirez, and R. Mackay, Al–*Si Alloys* (Springer, Cham, 2017). https://doi.org/10.1007/978-3-319-58380-8
8. N. A. Grishchenko, S. B. Sidel'nikov, and I. Yu. Gubanov, *Mechanical Properties of Aluminum Alloys* (Sib. Fed. Univ., Krasnoyarsk, 2012), p. 196.
9. A. P. Laskovnev, Yu. F. Ivanov, and E. A. Petrikova, *Modification of the Structure and Properties of Eutectic Silumin by Electron-Ion-Plasma Processing* (Navuka, Minsk, 2013). https://doi.org/10.31772/2587-6066-2021-22-2-371-382
10. A.T. Volochko, Lit'e Metall. **4**, 39 (2015).
11. R. Ren and D. Wei. Wang, Huang, and H. Zhang, Nucl. Instrum. Methods Phys. Res., Sect. B **505**, 44 (2021).
12. F. Xu, G. Tang, G. Guo, X. Ma, and G. Ozur, Nucl. Instrum. Methods Phys. Res., Sect. B **268**, 2395 (2010). https://doi.org/10.1016/j.nimb.2010.04.019
13. A. B. Belov, *High-Current Pulsed Electron Beams for Aircraft Engine Building* (Dipak, Moscow, 2012) [in Russian].
14. *Electron-Ion-Plasma Modification of the Surface of Nonferrous Metals and Alloys*, Ed. by N. N. Koval' and Yu. F. Ivanov (Nauchno-Tech. Lit., Tomsk, 2016) [in Russian].
15. J. Barrirero, *Eutectic Modification of Al-Si Casting Alloys* (Linköping Univ., Linköping, 2019). https://doi.org/10.3384/diss.diva-160235
16. V. Fedun and Yu. Kolyada, Vopr. At. Nauki Tekh., No. 7, 316 (2010).
17. S. Bratushka and L. V. Malikov, Vopr. At. Nauki Tekh., Ser.: Vak., Chist. Mater., Sverkhprovodn., No. 6, 126 (2011).
18. A. Andrianova, B. Borisov, E. Krit, M. Mashkova, M. Ovchinnikov, Timofeev, and F. Umarov, J. Phys.: Conf. Ser. **1713**, 012006 (2020). https://doi.org/10.1088/1742-6596/1713/1/012006
19. Yu. Ivanov, A. Klopotov, A. Potekaev, N. Koval, and V. Vlasov, IOP Conf. Ser.: Mater. Sci. Eng. **168**, 012070. (2017). https://doi.org/10.1088/1757-899X/168/1/012070
20. Yu. Ivanov, A. Klopotov, A. Potekaev, N. Koval, and V. Vlasov, IOP Conf. Ser.: Mater. Sci. Eng. **168**, 012070. (2017). https://doi.org/10.1088/1757-899X/168/1/012070
21. *Electron-Ion-Plasma Modification of the Surface of Nonferrous Metals and Alloys*, Ed. by N. N. Koval' and Yu. F. Ivanov (Nauchno-Tech. Lit., Tomsk, 2016) [in Russian].
22. V. E. Gromov, D. V. Zagulyaev, Yu. F. Ivanov, S. V. Konovalov, S. A. Nevskii, V. D. Sarychev, E. A. Budovskikh, and Yu. A. Rubannikova, *Structure and Hardening of Silumin Modified by Electron-Ion Plasma* (Sib. Gos. Ind. Univ., Novokuznetsk, 2020).
23. B. J. Inkson, *Materials Characterization using Nondestructive Evaluation (NDE) Methods* (Elsevier, Amsterdam, 2016), p. 17.
24. S. Primig, F. Theska, and N. Haghdadi, in *Electron Microscopy Methods* (Elsevier, Amsterdam, 2020). https://doi.org/10.1016/B978-0-12-819726-4.00031-4
25. J. Kuo, *Electron Microscopy: Methods and Protocols* (Humana, Totowa, 2014). https://doi.org/10.1007/978-1-62703-776-1
26. C. Qiuzi, Y. Xiang, and H. Li, in *Multifunctional Two- and Three-Dimensional Polycrystalline X-Ray Diffractometry* (Bentham, London, 2012), p. 34. https://doi.org/10.2174/97816080507651110101

Translated by L. Mosina